INNOVATIONS IN MOLECULAR BIOTECHNOLOGY
Jul-Dec 2025, VOL. 3, ISSUE 2, pp. 27-38
https://doi.org/10.61577/imb.2025.1000010

RESEAPRO JOURNALS

ORIGINAL ARTICLE

OPEN ACCESS

Evaluation of metal tolerance of bacterial strain isolated from Hooghly River coast soil

Shritika Bajpai

Department of Biotechnology, Utkal University, Odisha, India

ABSTRACT

The mangrove soils of the Sundarbans represent metal-rich, ecologically dynamic environments that support diverse microbial populations with potential applications in bioremediation. Heavy metal-tolerant bacteria from such habitats possess adaptive physiological mechanisms that enable survival under environmental stress. This study aimed to isolate and characterize bacterial strains capable of tolerating multiple heavy metals from mangrove soils of Sundarbans, West Bengal, India. Soil samples from five stations were processed using enrichment techniques to isolate Gram-positive and Gram-negative bacteria. Sixteen predominant and morphologically distinct isolates were selected for characterization. Heavy metal tolerance was evaluated against $ZnSO_4$, $CuSO_4$, $MnSO_4$, Pb, $HgCl_2$, $CoCl_2$, and K_2CrO_4 across increasing concentrations. Antibiotic susceptibility was evaluated, and the activities of stress-related enzymes such as catalase, peroxidase, polyphenol oxidase, ascorbate peroxidase, and ascorbic acid oxidase were assessed. The isolates exhibited varied tolerance profiles, sustaining 50–200 ppm of $ZnSO_4$, $CuSO_4$, $MnSO_4$, and Pb, but only 1–40 ppm of $HgCl_2$ and 5–100 ppm of $CoCl_2$. Strain MS-8 demonstrated the broadest tolerance range and was identified as Klebsiella aerogenes strain Ka37751.Most isolates were sensitive to tested antibiotics, except for resistance observed against Nystatin. The findings highlight diverse adaptive responses, reflected in differential enzyme activities and metal tolerance capacities. The study was limited by the number of isolates and lacked molecular investigation of resistance mechanisms. To identify metal-tolerant bacterial strains and evaluate their potential utility in bioremediation.

KEY WORDS

Metal tolerance; Bioremediation; Gram positive bacteria; Gram negative bacteria; Heavy metals

ARTICLE HISTORY

Received 20 November 2025;
Revised 11 December 2025;
Accepted 18 December 2025

Introduction

Heavy metals constitute a specific category of elements characterized by a density beyond 5 g/cm³. These metals persist in the environment due to their non-biodegradable nature and tend to accumulate through the food chain, resulting in long-term ecological and biological impacts [1]. While certain metals such as nickel, iron, copper, and zinc are essential micronutrients that serve as cofactors or structural components in vital metabolic reactions, others particularly mercury, silver, and cadmium are non-essential and toxic even at very low concentrations [2]. Their toxicity arises from their ability to disrupt cellular processes, interfere with enzymatic systems, and bind to essential biomolecules. Over the years, the concentration of these metals in natural habitats has increased significantly, primarily due to anthropogenic activities such as mining, industrial discharge, agricultural runoff, combustion of fossil fuels, and improper waste disposal.

The growing presence of heavy metals in various ecosystems has led to profound alterations in ecological balance, microbial diversity, and nutrient cycling. Mangrove ecosystems have emerged as critical sinks for metal contamination [3,4]. Although naturally rich in microbial communities, mangrove sediments now face increasing metal loads from urbanization, industrial effluents, and inadequate waste management. Heavy metals such as arsenic, cadmium, molybdenum, selenium, and zinc are frequently released in considerable quantities from coal and petroleum combustion, while lead contamination remains widespread due to deteriorating infrastructure, paints, automobile emissions, and environmental dust [5]. As a result, mangrove soils experience both environmental stress and microbial community shifts, affecting their overall resilience and ecological functioning.

Despite the inherent toxicity of elevated metal concentrations, mangrove sediments continue to harbor diverse microbial populations capable of adapting to such extreme environments. Metal-tolerant bacteria within these ecosystems have evolved various physiological, biochemical, and genetic mechanisms to withstand the adverse effects of metal exposure. These microbes not only survive but often play an essential role in maintaining soil health by participating in nutrient cycling, organic matter decomposition, and plant–microbe interactions [6,7]. Their capacity to immobilize, transform, or detoxify metals positions them as key contributors to the natural attenuation of contaminants. The overlap between metal resistance and antibiotic resistance has also garnered scientific attention, as both traits are frequently encoded on the same mobile genetic elements [8-10]. Consequently, prolonged metal exposure can indirectly co-select for antibiotic-resistant strains, raising concerns about environmental reservoirs of resistance.

Research on metal-tolerant bacteria has largely focused on isolating organisms from contaminated soils, sediments, industrial effluents, and wastewater. Standard methodologies often include the use of enrichment media to favor metal-adapted microorganisms, followed by morphological, biochemical, and molecular characterization [11]. Heavy metal tolerance is typically evaluated by determining the maximum tolerable concentration of specific metals, while enzyme

***Correspondence:** Ms. Shritika Bajpai, Department of Biotechnology, Utkal University, Odisha, India, e-mail: shritikabajpai16@gmail.com

assays help elucidate physiological responses under stress [12, 13]. Advanced techniques such as genome sequencing and proteomics further reveal the underlying mechanisms governing metal resistance or tolerance. However, despite substantial progress, comprehensive studies integrating both physiological and ecological assessments remain limited, particularly in mangrove ecosystems.

Existing literature demonstrates that metal-tolerant bacteria possess diverse strategies to withstand heavy metal toxicity. These mechanisms include efflux pumps, metal sequestration, enzymatic detoxification, and alterations in cell wall structure. Mangrove-associated microbes have been shown to promote plant growth under metal stress, enhance nutrient availability, and facilitate phytoremediation by reducing metal bioavailability. Studies further report that microbial diversity in metal-contaminated soils often shifts toward resistant populations, with measurable changes in biomass and metabolic activity. Such findings collectively highlight the ecological relevance and biotechnological potential of metal-tolerant bacteria in mitigating contamination [14].

Although substantial research exists on the adverse effects of heavy metals on susceptible microorganisms, relatively few studies have explored the physiological responses and adaptive mechanisms of metal-tolerant strains in detail. Most investigations rely on culture-dependent approaches, which may underestimate microbial diversity due to the uncultivability of many environmental microbes [15,16]. In addition, variations in environmental conditions such as pH, organic matter content, speciation of metals, and presence of chelating agents can significantly influence microbial responses, making cross-study comparisons difficult. Furthermore, comprehensive genomic and molecular analyses required to fully elucidate resistance mechanisms remain scarce in the context of mangrove ecosystems.

Given these gaps, the present research aims to systematically isolate and characterize metal-tolerant bacteria from mangrove soils of the Sundarbans and evaluate their tolerance to different heavy metals. The study further intends to examine their physiological and enzymatic responses under metal stress, assess their potential interactions with antibiotics, and identify strains with promising applications in bioremediation [17]. Through this approach, the research seeks to contribute to a deeper understanding of microbial adaptation in metal-contaminated environments and highlights the potential of native bacterial isolates in restoring ecological balance in mangrove ecosystems (Table 1).

Table 1. The different metals causing pollutionalong with their source and effects on living organisms.

Metals	Source	Effect on living organisms
Mercury	Batteries, coal, combustion, mining,paint industries, paper industry	Ataxia, kidney problems, memory loss etc.
Zinc Sulphate	Brass, oil refinery, plumbing,mining.	Ataxia, depression, prostate cancer, affect photosynthesis, reduced growth rate.
Copper Sulphate	In soil it may originate from natural sources, pesticides, or other sources.These may include mining, industry, architectural material, and motor vehicles.	Copper sulphate can irritate the eyes severely. Consuming a lot of copper sulphate can cause nausea, vomiting, and other symptoms.
Potassium dichromate	Potassium dichromate is found naturally in our environment, in sand, ash, clay, and loam. It can be found in tools made of steel, and chrome-plated objects (silverware, handles, bracelets, needles, etc.).	May cause an allergy or asthma symptoms or breathing difficulties if inhaled.
Manganese Sulphate	A byproduct of several important commercial oxidations involving manganese dioxide, such as the production of hydroquinone and anisaldehyde, is manganese sulphate.	Neurologic effects, forgetfulness, anxiety, or insomnia.
Cobalt Chloride	In spray paints, enamels, wood stains and paints,as well as bricks and cement and metal tools.	Excess dietarycobalt produces toxic effects in animals.
Lead Acetate	Coal combustion, paint, mining, batteries, electroplating.	Chronic kidney damage, memory problems, enzymesand nucleic acid damage, chlorosis inplants, reduced photosynthesis.

Materials and Methods

Isolation of bacteria

One gram of each soil sample was serially diluted in 9 g of sterile distilled water (121 °C, 15 min) up to 10^{-6}. Nutrient agar (NA) plates (2.8 g/100 mL) were prepared, solidified, and inoculated with 0.1 µL of each dilution using a sterile L-spreader. The plates were appropriately labeled and incubated in a BOD incubator at 30 ± 0.1 °C for 24 hours. After incubation, colonies displaying distinct morphological characteristics were randomly selected and streaked on fresh NA plates to obtain pure single colonies. These purified isolates were subsequently transferred to NA slants for maintenance and further analysis.

Composition of nutrient agar plate

Nutrient agar (NA) medium was made by dissolving 28 g of NA powder in 1000 mL of distilled water, or 2.8 g per 100 mL. As the isolated bacteria exhibited salt tolerance, the medium was supplemented with an additional 0.5% NaCl to support optimal growth. The components were thoroughly mixed and subsequently processed for sterilization and use in bacterial cultivation.

Staining methods

Gram staining was conducted to determine whether the isolates were Gram-positive or Gram-negative. Fresh bacterial cultures (8–12 h old) were smeared onto clean glass slides,

https://doi.org/10.61577/imb.2025.1000010

air-dried, and heat-fixed by briefly passing over a flame. After staining the smears with crystal violet for a minute, they were rinsed and then treated with Gram's iodine for another minute. After washing, the slides were decolorized using 95% ethanol and immediately rinsed again. A counterstain of safranin was applied for 30 seconds, followed by a final wash and air-drying. The stained cells were examined microscopically under a 100× oil immersion objective with a daylight filter.

Oxidase test

Oxidase activity was assessed by incubating bacterial cultures in nutrient broth at 30 °C for 72 hours, followed by the addition of 0.2% methylene blue. Decolorization of the broth indicated a positive reaction, with a control maintained for comparison.

Catalase test

Catalase activity was evaluated by flooding overnight NA-grown bacterial cultures with 1% hydrogen peroxide. Immediate effervescence indicated a positive reaction, confirming the enzymatic breakdown of hydrogen peroxide.

Indole production test

The indole test was performed by inoculating bacterial cultures into tryptone broth and incubating at 30 ± 0.1 °C for 72 hours. Following incubation, Kovac's reagent was added, and indole production was indicated by a pink ring at the interface, while its absence signified a negative result.

Methyl Red test

The methyl red test was performed by inoculating bacteria into MRVP broth and incubating at 30 ± 0.1 °C for 72 hours. After incubation, alcoholic methyl red indicator was added, and a red coloration indicated acid production, while the prepared indicator solution contained 0.1 g methyl red in ethanol and distilled water.

Voges-proskauer (Acetoin production) test

The Voges–Proskauer test was conducted by inoculating bacteria into MRVP broth and incubating at 30 ± 0.1 °C for 72–96 hours. After incubation, α-naphthol and KOH were added, and development of a crimson-red color indicated acetoin production, while absence of color change denoted a negative reaction.

Citrate utilization test

Citrate utilization was assessed using Simmon's citrate agar slants incubated at 30 ± 0.1 °C for 96 hours. Growth accompanied by a color change from green to blue indicated a positive result, whereas absence of growth and retention of the yellowish-green color signified a negative reaction.

Indicator: Bromothymol blue (10 mg) was dissolved in 0.25 mL of 1 N NaOH and diluted with 4.75 mL of distilled water.

Nitrate reduction test

Nitrate reduction was assessed by inoculating bacteria into nitrate broth and incubating at 30 ± 0.1 °C for 96 hours. After incubation, a 1:1 mixture of sulphanillic acid and α-naphthylamine was added, with deep pink coloration indicating a positive reaction; non-reactive cultures were diluted and retested.

Reagent

Solution A: Sulphanillic acid 8 g dissolved in 1 l 5 N acetic acid (glacial acetic acid: water: 1:2.5).

Solution B: α –naphthylamine 5 g dissolved in 1 litre 5 N acetic acid.

Equal volumes of solution A and B were mixed before use.

Hydrogen sulphide (H_2S) production test

Hydrogen sulfide production was detected using lead acetate–impregnated filter paper strips sterilized and dried at 120 °C. Strips were inserted into inoculated culture tubes and incubated at 20 ± 0.1 °C for 7 days. Blackening of the strip due to ferrous sulfide formation indicated a positive reaction.

Carbohydrate fermentation (Acid production) and utilization test

Carbohydrate and glycoside fermentation, as well as starch and aesculin utilization, were assessed on basal medium plates containing bromocresol purple. Cultures were spot-inoculated and incubated for 72 hours. Acid production caused a color change to yellow or violet-purple, while aesculin hydrolysis produced darkened colonies. Sterile substrates and indicators were filter-added before plating, and plates were examined daily.

Carbohydrate metabolism (acid-gas production) test

Carbohydrate fermentation was assessed by inoculating bacteria into nutrient broth containing 1% filter-sterilized sugars, bromothymol blue, and an inverted Durham tube, followed by incubation at 30 ± 0.1 °C for 72 hours. Acid production caused yellow coloration, while gas formation was indicated by bubbles trapped in the Durham tube.

Tween 80 hydrolysis test

The ability of the microorganisms to hydrolyze Tween-80 into fatty acids and glycerol is assessed in the test. Fatty acid reacts with Ca present in the medium and forms an opaque zone around the colonies.

Tributarily hydrolysis test

Lipase activity was assessed on tributyrin (or vegetable oil)–containing medium, where the emulsified substrate produced opacity. Lipase-producing organisms hydrolyzed the substrate into water-soluble butyric acid, forming clear zones around colonies, indicating a positive reaction.

Casein hydrolysis test

Casein hydrolysis was evaluated on NA plates containing 1% casein, spot-inoculated and incubated at 30 °C for 24–48 hours. Plates were then flooded with 15% acidic $HgCl_2$, and clear zone formation indicated proteolytic activity. The ratio of clear zone diameter to colony growth reflected enzymatic efficiency.

Starch hydrolysis test

Starch hydrolysis was assessed by spot inoculating bacterial cultures onto NA plates containing 1% soluble starch and incubating at 30 ± 0.1 °C for 24 hours. Plates were flooded with iodine solution, and complete or partial starch degradation was indicated by clear or reddish-brown zones surrounding the colonies.

Effect of Salinity

Salinity effects were assessed using NaCl concentrations ranging from 1–12%. Enzyme solution, buffer, and 0.2% starch were incubated at optimal temperature, after which the

https://doi.org/10.61577/imb.2025.1000010

reaction was terminated with acetic acid and iodine. Absorbance was measured at 690 nm to determine enzyme activity under varying salinity.

Effect of Heavy Metals

Magnesium: The effect of Mg^{2+} on enzyme activity was evaluated by incubating enzyme solution, buffer, and 0.2% starch with Mg salt concentrations of 10–70 ppm. Reactions were stopped with acetic acid and iodine, and hydrolysis was measured at 690 nm. Amylase activity was expressed as µmol of reducing sugars released per minute per gram.

Copper: The effect of Cu^{2+} on amylase activity was assessed by incubating enzyme solution, buffer (pH 7.0), and 0.2% starch with Cu salt concentrations of 10–90 ppm. Reactions were terminated with acetic acid and iodine, and hydrolysis was measured at 690 nm. Enzyme activity was expressed as µmol of reducing sugars released per minute per gram.

Iron: The effect of Fe^{2+} on amylase activity was evaluated by incubating enzyme solution, buffer, and 0.2% starch with Fe salt concentrations of 10–100 ppm. Reactions were terminated with acetic acid and iodine, and hydrolysis was measured at 690 nm. Enzyme activity was expressed as µmol of reducing sugars released per minute per gram.

Manganese: The effect of Mn^{2+} on amylase activity was assessed by incubating enzyme solution, buffer, and 0.2% starch with Mn salt concentrations of 10–100 ppm. Reactions were terminated with acetic acid and iodine, and hydrolysis was measured at 690 nm. Enzyme activity was expressed as µmol of reducing sugars released per minute per gram.

Antibiotics Susceptibility Testing

Antibiotic susceptibility was assessed using the CLSI-recommended Kirby–Bauer disc diffusion method. Bacterial inocula were adjusted to 0.5 McFarland standard and spread on Mueller–Hinton agar. After incubation at 37 °C for 24 hours, inhibition zones were measured and isolates classified as sensitive, intermediate, or resistant per CLSI guidelines.

Molecular Identification of Isolate MS-8

Among the eight isolates, MS-8 was identified as the most promising strain from the Sundarbans mangrove. Genomic DNA was extracted using the phenol–chloroform method and quantified by Nanodrop. The 16S rRNA gene was amplified, yielding a single purified band, and phylogenetic analysis using NCBI databases confirmed its identity. Morphological characterization showed MS-8 to be a rod-shaped, endospore-forming, Gram-positive bacterium.

Results and Discussion

Isolation and morphology of bacterial strains

A total of sixteen bacterial isolates were successfully obtained from soil and water samples collected from Dhanchi Forest, near the Hooghly River. Serial dilution and plating on nutrient agar yielded morphologically distinct colonies, which were purified and maintained for further characterization. The isolates displayed diverse pigmentation, colony forms, elevations, and surface textures, as shown in Figures 1 and 2. Microscopic examination revealed varied cell morphologies, predominantly rod-shaped and coccoid forms, with both Gram-positive and Gram-negative populations (Table 2 and Figure 3).

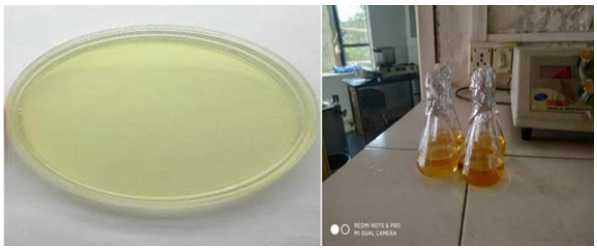

Figure 1. Preparation of pure culture media.

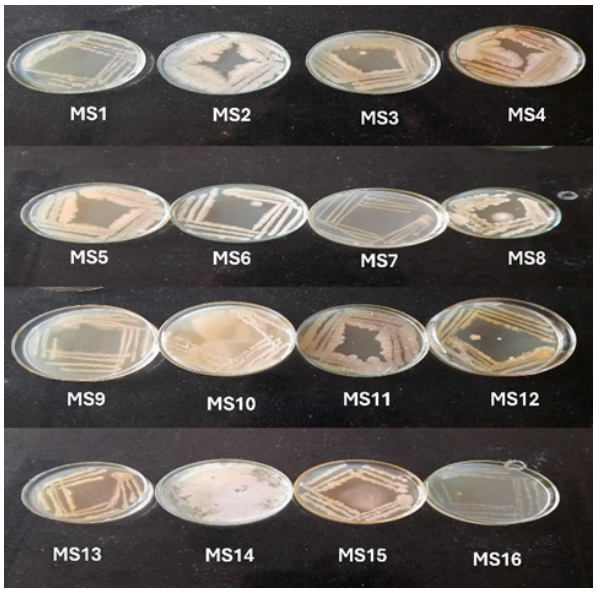

Figure 2. Pure culture of the isolates.

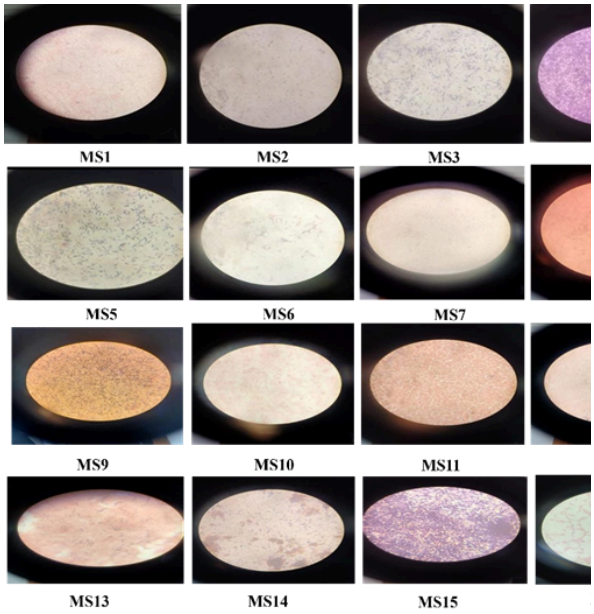

Figure 3. Microscopic view of all native bacterial strain.

https://doi.org/10.61577/imb.2025.1000010

Table 2. Morphological characters of native bacterial strains.

Sl. No. of Bacteria	Morphological characters
SB 1	Punctiform, Yellow,Opaque, Small colu, convex surface,Circular, Entire mucoid, Round, Monococci, Gram positive, Single smooth cell.
SB 2	Filamentous, Irregular, Opaque, Convex, Circular, Entire,White colour, large cell, Smooth round, Monocooci, Gram positive, Single cell mucoid.
SB 3	White colour,Irregular, Opaque, Smoothflat, Entire, Circular, Small colonies, Mucoid rod shape, Diplococcic, Two cells, Gram positive.
SB 4	Punifunetion, Opaque,Flat, Irregular, Mucoidentire, large colonies, Smooth single cell, Monococci, Spherical, Gram negative.
SB 5	White colour,Opaque, Flat, Circular,Trible large colonies,Entire, Circular, Smooth rod shape, Diplococci, Gram positive, Two cells.
SB 6	White colour,Opaque, Convex, Irregularmucoid, Entire small colonies, Smooth, Circular, Rod shape, Many cells, Gram positive, Streptococci, Chain of bacillus.
SB 7	Large colonies,Irregular, Circular, Entire,flat, Smooth, White colour, mucoid opaque, Gram negative, Rod shape, Single cell, Monococci.
SB 8	Large colonies,Irregular, Circular, Entire,flat, Smooth, White colour, mucoid opaque, Gram negative, Rod shape, Singlecell, Monococci.
SB 9	Large colonies,Irregular, Opaque filamentous, Entire, White colour,Smooth flat mucoid, Gram positive,Rod shape, Singlecells, Monococci.
SB 10	Large colonies,Irregular, Opaque filamentous, Entire, White colour,Smooth flat mucoid, Gram positive,Rod shape, Singlecells, Monococci.
SB 11	Large colonies,Round, Opaque, Flat, Mucoid moot, Entire, Irregular, Pale yellow, Gram negative, Single cells, Circular, Monococci.
SB 12	Large colonies, Irregular, Opaque, Mucoid concave, Entire, White colour, Rough, Gram positive,Single cells monococci, Rod shape.
SB 13	Small colonies, Irregular, Opaque, Flat miscid, Entire, White colour, Smooth, Circular, Gram positive, Chain of bacilli,many cells feel shape.
SB 14	Large colonies, Irregular opaque, round convex, Entire, Viscid, White colour,Smooth, Circular, Gram positive, Two cells diplococcic.
SB 15	Large colonies, Irregular, Circular, Entire, Convex, Smooth, White colour, mucoid,Opaque, Gram positive, Rod shape, Many cells, Chainof bacilli.
SB 16	Small colonies, Irregular, Round, Entire, Convex, Smooth, White colour, mucoid,Opaque, Gram positive,Oval, Single cells, Monococci.

Biochemical characterization

The isolates showed heterogeneous biochemical profiles, including variable activities for amylase, protease, lipase, cellulase, and phosphate solubilization (Figure 4 and Table 3). Carbohydrate fermentation patterns, citrate utilization, indole formation, and MR–VP results further differentiated the strains, confirming significant physiological diversity.

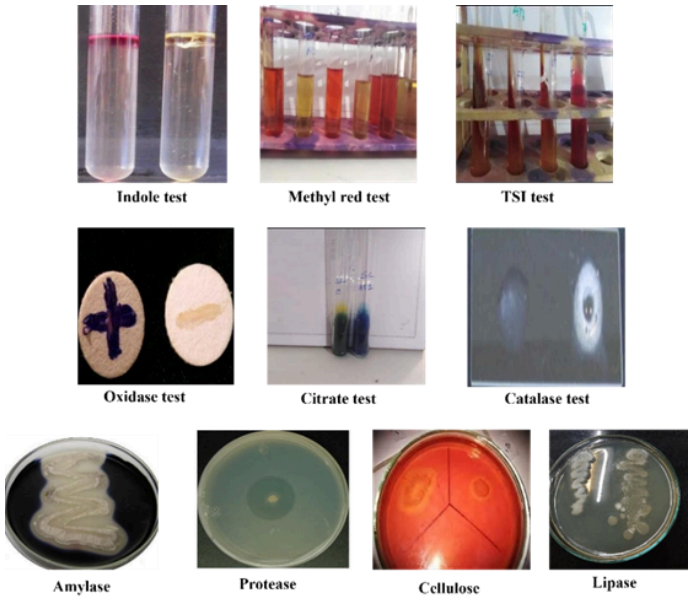

Figure 4. Biochemical analysis of 16 Bacterial strains.

https://doi.org/10.61577/imb.2025.1000010

Table 1. Biochemical characters of native bacterial strains.

SAMPLE NO.	Amalyase Test	Protease Test	Lipase Test	Phosphate Test	Cellulose Test (CMC)	Citarte Test	MR-VP Test	TSI Test	Indole Test	H_2O_2 Test	Oxidase Test
MS1	-	-	-	-	-	+++	-	A/A	+++	+++	+++
MS2	+++	+++	-	-	-	-	-	A/A	+++	-	-
MS3	+++	+++	-	-	+++	-	-	A/A	+++	+++	+++
MS4	+++	+++	+++	+++	+++	+++	-	K/A	+++	+++	+++
MS5	+++	+++	+++	-	+++	-	-	A/A	+++	-	+++
MS6	+++	+++	+++	+++	-	+++	-	K/A	+++	+++	-
MS7	-	-	+++	+++	+++	+++	-	A/A	-	+++	+++
MS8	+++	+++	-	-	+++	-	-	A/A	+++	+++	+++
MS9	+++	+++	+++	-	+++	+++	-	K/A	-	+++	+++
MS10	-	+++	+++	-	+++	+++	-	K/A	+++	+++	+++
MS11	+++	-	-	+++	+++	+++	-	K/A	+++	+++	+++
MS12	+++	-	-	-	-	+++	-	A/A	-	+++	-
MS13	-	+++	+++	+++	+++	+++	-	K/A	+++	+++	+++
MS14	-	-	+++	+++	+++	+++	-	A/A	-	+++	+++
MS15	+++	+++	-	-	-	-	-	A/A	-	+++	+++
MS16	-	-	-	-	+++	+++	-	K/A	+++	+++	+++

NaCl tolerance

Salt tolerance assays demonstrated that most isolates grew optimally at 3–6% NaCl, while only MS6, MS8, MS9, and MS11 tolerated up to 8% NaCl (Table 4 and Figure. 5). Growth was not observed at 10% NaCl for any strain.

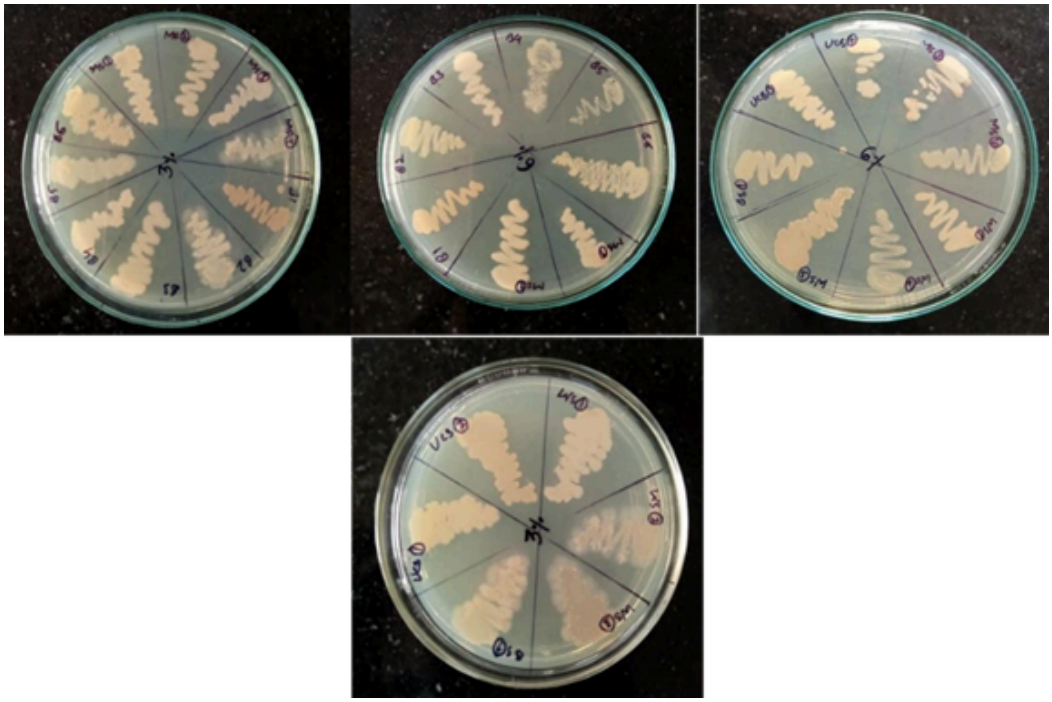

Figure 5. NaCl Tolerance.

Table 4. Nacl Tolerance.

SAMPLE	3%	6%	8%	10%
MS1	+++	+++	-	-
MS2	+++	+++	-	-
MS3	+++	+++	-	-

https://doi.org/10.61577/imb.2025.1000010

MS4	+++	+++	-	-
MS5	+++	+++	-	-
MS6	+++	+++	+++	-
MS7	+++	+++	-	-
MS8	+++	+++	+++	-
MS9	+++	+++	+++	-
MS10	+++	+++	-	-
MS11	+++	+++	+++	-
MS12	+++	+++	-	-
MS13	+++	+++	-	-
MS14	+++	+++	-	-
MS15	+++	+++	-	-
MS16	+++	+++	-	-

Antibiotic susceptibility

Kirby–Bauer assays revealed that the isolates were largely sensitive to gentamicin, tetracycline, streptomycin, and kanamycin, with small inhibition zones observed (Table 5 and Figure 6). MS8 and MS11 showed moderate resistance patterns but remained susceptible overall.

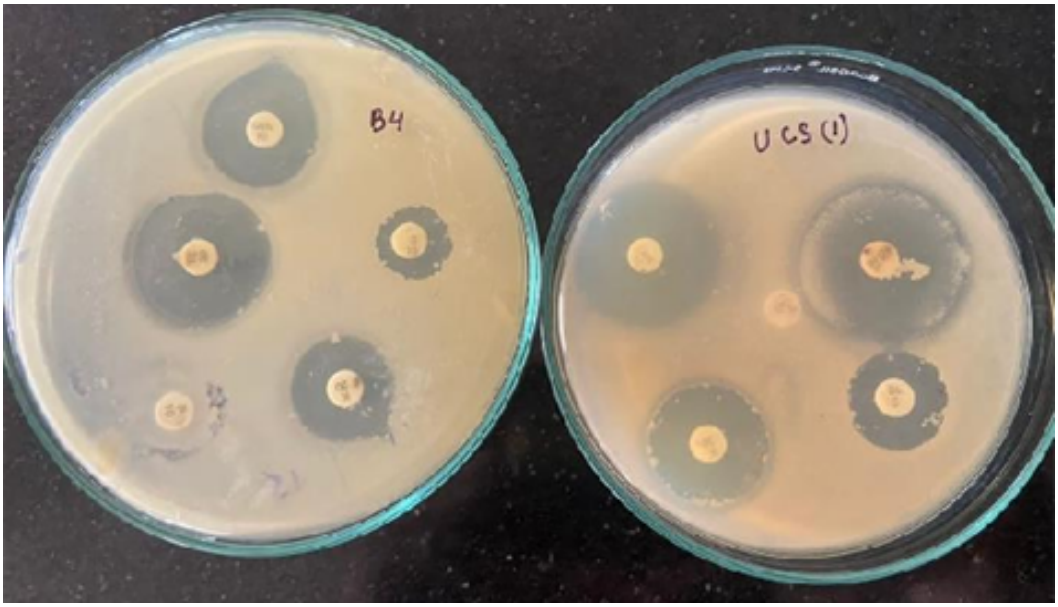

Figure 6. Antibiotic resistance.

Table 5. Result of antibiotic resistance test.

MS 11				**MS 8**			
GEN (10)	TE (30)	S (10)	K (30)	GEN (10)	TE (30)	S (10)	K (30)
1.2-0.5	1.1-0.5	0.5-.0	0.7-0.5	0.8-0.5	1.2-0.5	0.4-0.5	0.7-0.5
=0.7cm	=0.6cm	=0cm5	=0.2cm	=0.3cm	=0.3cm	=0.1cm	=0.2cm

Heavy metal tolerance

The isolates displayed varying tolerance across seven heavy metals.

Mercury ($HgCl_2$)

MS7, MS8, and MS12 exhibited the highest tolerance, sustaining growth up to 40 ppm $HgCl_2$ (Table 6 and Figure 7).

Table 6. Metal tolerance of $HgCl_2$.

Sample	**1PPM**	**2PPM**	**4PPM**	**5PPM**	**10PPM**	**20PPM**	**20PPM**	**40PPM**
MS1	+++	+++	+++	+++	+++	+++	+++	-
MS2	+++	+++	-	-	-	-	-	-

https://doi.org/10.61577/imb.2025.1000010

MS3	+++	+++	-	-	-	-	-	-
MS4	+++	+++	-	-	-	-	-	-
MS5	+++	+++	-	-	-	-	-	-
MS6	+++	+++	-	-	-	-	-	-
MS7	+++	+++	+++	+++	+++	+++	+++	+++
MS8	+++	+++	+++	+++	+++	+++	+++	+++
MS9	+++	+++	-	-	-	-	-	-
MS10	+++	+++	-	-	-	-	-	-
MS11	+++	+++	-	-	-	-	-	-
MS12	+++	+++	+++	+++	+++	+++	+++	+++
MS13	+++	+++	-	-	-	-	-	-
MS14	+++	+++	-	-	-	-	-	-
MS15	+++	+++	+++	+++	+++	+++	+++	-
MS16	+++	+++	+++	+++	+++	+++	+++	-

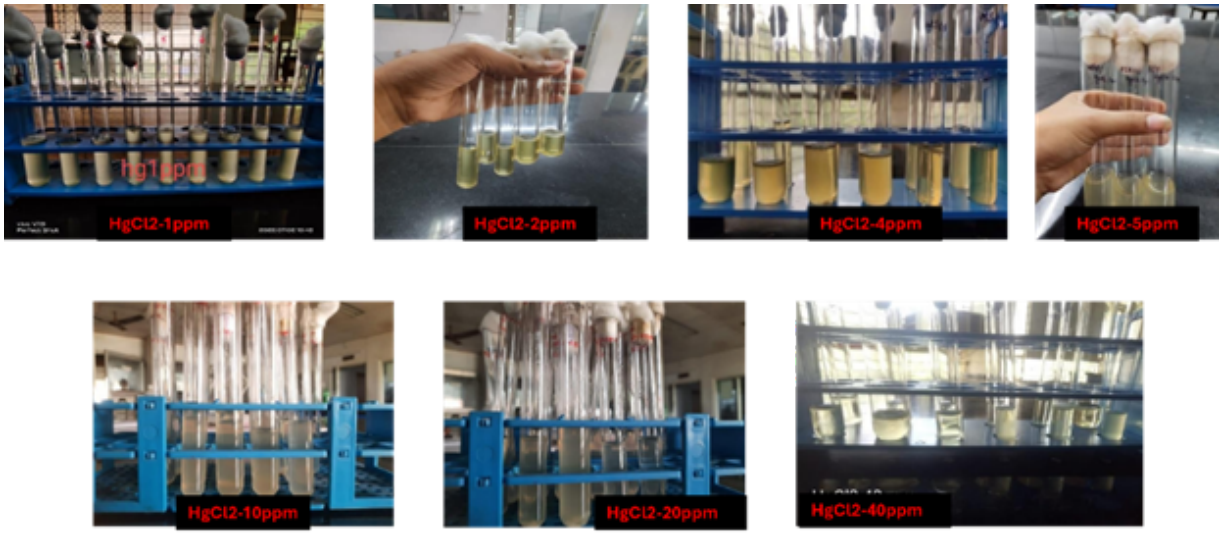

Figure 7. Metal tolerance of $HgCl_2$.

Zinc ($ZnSO_4$)

Most strains tolerated 50–100 ppm $ZnSO_4$, while only MS8 sustained growth at 200 ppm (Table 7 and Figure 8).

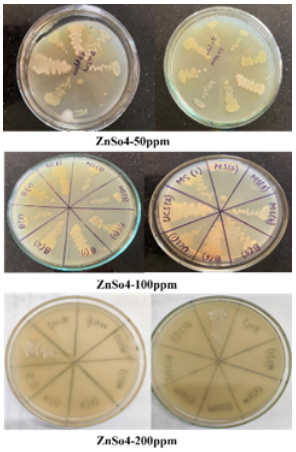

Figure 8. Biochemical result of $ZnSo_4$.

Table 7. Biochemical resultof ZnSO4 in 50, 100 and 200ppm.

Sample	50 PPM	100 PPM	200PPM
MS1	+++	+++	-
MS2	+++	+++	-
MS3	+++	+++	-
MS4	+++	+++	-
MS5	-	+++	+++
MS6	+++	+++	-
MS7	+++	+++	-
MS8	+++	+++	+++
MS9	+++	+++	-
MS10	+++	+++	-
MS11	+++	+++	-
MS12	+++	+++	-
MS13	+++	+++	-
MS14	-	+++	-
MS15	-	+++	-
MS16	+++	+++	-

https://doi.org/10.61577/imb.2025.1000010

Copper ($CuSO_4$)

Remarkably, MS8 was the only isolate capable of tolerating 50–200 ppm $CuSO_4$ (Table 8).

Table 8. Biochemical results of CuSo4 in 50,100 and 200 ppm.

Sample	50 PPM	100 PPM	200PPM
MS1	-	-	-
MS2	-	-	-
MS3	-	-	-
MS4	-	-	-
MS5	-	-	-
MS6	-	-	-
MS7	-	-	-
MS8	+++	+++	+++
MS9	-	-	-
MS10	-	-	-
MS11	-	-	-
MS12	-	-	-
MS13	-	-	-
MS14	-	-	-
MS15	-	-	-
MS16	-	-	-

Potassium Dichromate ($K_2Cr_2O_7$)

All isolates grew at 50–100 ppm, and strong tolerance (+++) was observed at 200 ppm (Table 9 and Figure 9).

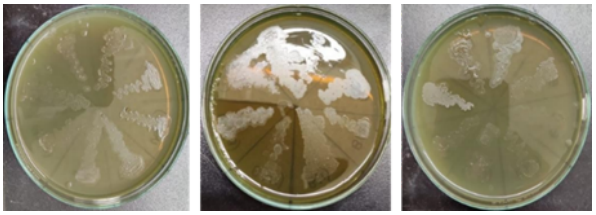

Figure 9. Biochemical resultsof $K_2Cr_2O_7$.

Table 9. Biochemical resultsof $K_2Cr_2O_7$.

Sample	50 PPM	100 PPM	200PPM
MS1	++	++	+++
MS2	++	++	+++
MS3	++	++	+++
MS4	++	++	+++
MS5	++	++	+++
MS6	++	++	+++
MS7	++	++	+++
MS8	++	++	+++
MS9	++	++	+++
MS10	++	+++	+++
MS11	++	+++	+++
MS12	++	+++	+++
MS13	++	+++	+++
MS14	++	+++	+++
MS15	++	+++	+++
MS16	++	+++	+++

Manganese ($MnSO_4$)

All isolates showed uniform and robust tolerance up to 200 ppm $MnSO_4$ (Table 10, Figure 10).

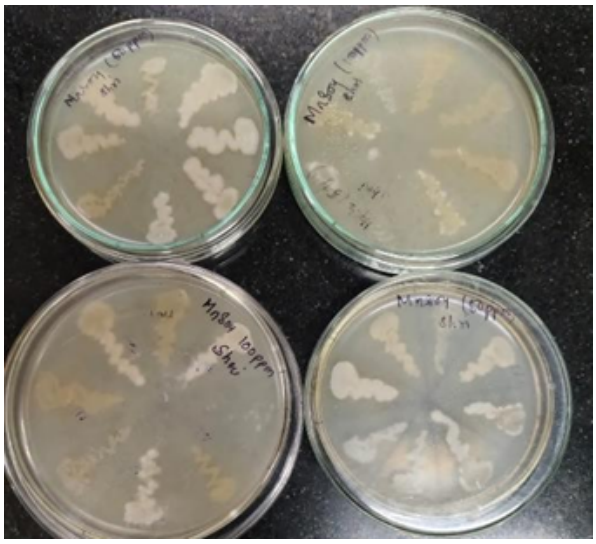

Figure 10. MnSo4 at 50ppm & 100ppm.

Table 10. Biochemical resultsof $MnSO_4$.

Sample	50 PPM	100 PPM	200PPM
MS1	+++	+++	+++
MS2	+++	+++	+++
MS3	+++	+++	+++
MS4	+++	+++	+++
MS5	+++	+++	+++
MS6	+++	+++	+++
MS7	+++	+++	+++
MS8	+++	+++	+++
MS9	+++	+++	+++
MS10	+++	+++	+++
MS11	+++	+++	+++
MS12	+++	+++	+++
MS13	+++	+++	+++
MS14	+++	+++	+++
MS15	+++	+++	+++
MS16	+++	+++	+++

Cobalt ($CoCl_2$)

MS8 showed the highest tolerance, growing even at 100 ppm, while other isolates were inhibited above 50 ppm (Table 11, Figure 11).

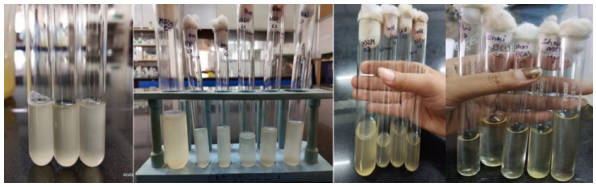

Figure 11. $CoCl_2$ at 5ppm, 10ppm, 50ppm & 100ppm.

https://doi.org/10.61577/imb.2025.1000010

Table 11. Biochemical resultof $Cocl_2$.

Sample	5 PPM	10 PPM	50PPM	100PPM
MS1	+++	+++	++	-
MS2	+++	10 PPM	++	-
MS3	5 PPM	+++	++	-
MS4	+++	+++	++	-
MS5	+++	+++	++	-
MS6	+++	+++	++	-
MS7	+++	+++	++	-
MS8	+++	+++	+++	+++
MS9	+++	+++	++	-
MS10	+++	+++	++	-
MS11	+++	+++	++	-
MS12	+++	+++	++	-
MS13	+++	+++	++	-
MS14	+++	+++	++	-
MS15	+++	+++	++	-
MS16	+++	+++	++	-

Lead Acetate (Pb)

Most isolates tolerated 50–100 ppm Pb, but only MS8 demonstrated strong growth at 200 ppm (Table 12 and Figure 12).

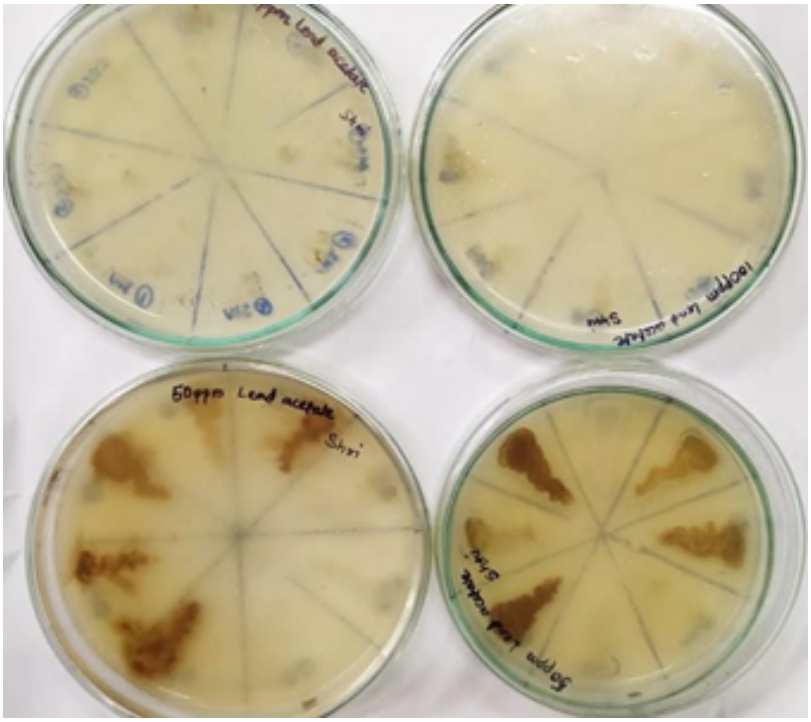

Figure 12. Lead acetate at 50ppm & 100ppm

Table 12. Biochemical results of Lead acetate

Sample	50 PPM	100 PPM	200PPM
MS1	+++	++	-
MS2	+++	++	-
MS3	+++	++	-

https://doi.org/10.61577/imb.2025.1000010

MS4	+++	++	-
MS5	+++	++	-
MS6	+++	++	-
MS7	+++	++	-
MS8	+++	+++	++
MS9	+++	++	-
MS10	+++	++	-
MS11	+++	++	++
MS12	+++	++	++
MS13	+++	++	-
MS14	+++	++	-
MS15	+++	++	-
MS16	+++	++	-

MIC summary

Minimal inhibitory concentration data clearly identified MS8 as the most metal-tolerant strain across all tested metals (Table 13).

Table 13. MIC values of Bacterial isolates against different concentrations of metals.

Metals	PPM	MS1	MS2	MS5	MS8	MS10	MS13	MS14	MS15	MS16
HG	1PPM	+++	+++	+++	+++	MS10	+++	+++	+++	+++
	2PPM	+++	+++	+++	+++	MS10	+++	+++	+++	+++
	4PPM	+++	-	-	+++	-	-	-	+++	+++
	5PPM	+++	-	-	+++	-	-	-	+++	+++
	10PPM	+++	-	-	+++	-	-	-	+++	+++
	20PPM	+++	-	-	+++	-	-	-	+++	+++
	40PPM	-	-	-	+++	-	-	-	-	-
CO	5PPM	+++	+++	+++	+++	+++	+++	+++	+++	+++
	10PPM	+++	+++	+++	+++	+++	+++	+++	+++	+++
	50PPM	++	++	++	+++	++	++	++	++	++
	100PPM	-	-	-	+++	-	-	-	-	-
$ZnSo_4$	50PPM	+++	+++	-	+++	+++	+++	-	-	+++
	100PPM	+++	+++	+++	+++	+++	+++	+++	+++	+++
	200PPM	-	-	-	+++	-	-	-	-	-
$MnSo_4$	50PPM	+++	+++	+++	+++	+++	+++	+++	+++	+++
	100PPM	+++	+++	+++	+++	+++	+++	+++	+++	+++
	200PPM	+++	+++	+++	+++	+++	+++	+++	+++	+++
Pb	50PPM	+++	+++	+++	+++	+++	+++	+++	+++	+++
	100PPM	++	++	++	++	++	++	++	++	++
	200PPM	-	-	-	+++	-	-	-	-	-
$K_2Cr_2O_7$	50PPM	++	++	++	+++	++	++	++	++	++
	100PPM	++	++	++	+++	+++	+++	+++	+++	+++
	200PPM	+++	+++	+++	+++	+++	+++	+++	+++	+++
$CuSo_4$	50PPM	-	-	-	+++	-	-	-	-	-
	100PPM	-	-	-	+++	-	-	-	-	-
	200PPM	-	-	-	+++	-	-	-	-	-

Here +++ denotes to strongly positive & ++ denotes to slightly positive.

Molecular identification of MS-8

Genomic DNA extracted from MS8 showed a clear high-molecular-weight band (Fig. 31). PCR amplification yielded a ~1500 bp 16S rRNA fragment, which upon sequencing revealed 99% identity with Klebsiella aerogenes. Phylogenetic analysis placed the isolate firmly within the K. aerogenes cluster (Figure 13). Morphological observations confirmed MS8 as a

https://doi.org/10.61577/imb.2025.1000010

rod-shaped, Gram-negative bacterium.

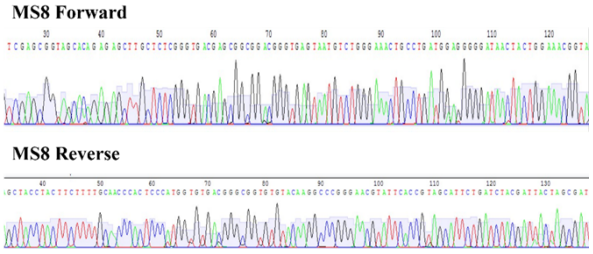

Figure 1. Dendogram of sequenceof MS-8.

Conclusion

The present study focused on the isolation and characterization of halo-tolerant, metal-resistant bacteria from the mangrove soils of the Sundarbans, West Bengal—an ecosystem recognized for its fluctuating salinity and increasing exposure to heavy metal contaminants. A total of sixteen bacterial isolates were obtained and initially selected based on their ability to grow under elevated NaCl concentrations. These isolates were subsequently assessed for their tolerance to a range of heavy metals, including mercury ($HgCl_2$), copper ($CuSO_4$), zinc ($ZnSO_4$), cobalt ($CoCl_2$), manganese ($MnSO_4$), lead acetate (Pb), and potassium dichromate ($K_2Cr_2O_7$), across increasing concentrations.

Metal tolerance profiling through minimum inhibitory concentration (MIC) assays revealed significant variability among the isolates, indicating diverse physiological adaptations to metal stress within the mangrove microbial community. Among all the tested strains, isolate MS-8 consistently exhibited the highest degree of resistance to all seven metals, with sustained growth even at concentrations as high as 200 ppm for several metals. This broad-spectrum tolerance demonstrates the exceptional resilience of MS-8 and suggests the presence of efficient metal-detoxifying or metal-regulating mechanisms.

Molecular identification via 16S rRNA gene sequencing confirmed MS-8 as Klebsiella aerogenes strain Ka37751. The strain's strong halotolerance, combined with its pronounced metal resistance, highlights its ecological significance and potential applicability in bioremediation strategies aimed at restoring heavy metal–contaminated environments. Given the increasing anthropogenic pressures on sensitive coastal ecosystems such as the Sundarbans, microbial strains like MS-8 may serve as valuable biological resources for sustainable remediation practices.

Overall, this study establishes that Sundarbans mangrove soils harbor microorganisms with substantial metal tolerance capacities. The findings underscore the importance of exploring native microbial diversity for environmentally compatible, biologically driven approaches to heavy metal mitigation and ecosystem rehabilitation.

Disclosure Statement

No potential conflict of interest was reported by the author.

References

1. Ali H, Khan E, Ilahi I. Environmental chemistry and ecotoxicology of hazardous heavy metals: environmental persistence, toxicity, and bioaccumulation. J Chem. 2019;2019(1):6730305. https://doi.org/10.1155/2019/6730305
2. Bibi M, Samiullah FB, Saba Afzal S. Essential and non-essential heavy metals sources and impacts on human health and plants. Pure appl biol. 2023;12(2):835-847. https://doi.org/10.19045/bspab.2023.120083
3. Puthusseri RM, Nair HP, Johny TK, Bhat SG. Insights into the response of mangrove sediment microbiomes to heavy metal pollution: Ecological risk assessment and metagenomics perspectives. J Environ Manage. 2021;298:113492. https://doi.org/10.1016/j.jenvman.2021.113492
4. Koka EG, Masao CA, Limbu SM, Kilawe CJ, Norbert J, Pauline NM, Perfect J, Mabhuye EB. A systematic review on distribution, sources and impacts of heavy metals in mangrove ecosystems. Mar Pollut Bull. 2025;213:117666. https://doi.org/10.1016/j.marpolbul.2025.117666
5. Ali MM, Hossain D, Khan MS, Begum M, Osman MH. Environmental pollution with heavy metals: A public health concern. InHeavy metals-their environmental impacts and mitigation 2021. https://doi.org/10.5772/intechopen.96805
6. Nnaji ND, Anyanwu CU, Miri T, Onyeaka H. Mechanisms of heavy metal tolerance in bacteria: A review. Sustainability. 2024;16(24):11124. https://doi.org/10.3390/su162411124
7. Tiwari S, Lata C. Heavy metal stress, signaling, and tolerance due to plant-associated microbes: an overview. Front Plant Sci. 2018;9:452. https://doi.org/10.3389/fpls.2018.00452
8. Gillieatt BF, Coleman NV. Unravelling the mechanisms of antibiotic and heavy metal resistance co-selection in environmental bacteria. FEMS Microbiol Rev. 2024;48(4):fuae017. https://doi.org/10.1093/femsre/fuae017
9. Pal C, Asiani K, Arya S, Rensing C, Stekel DJ, Larsson DJ, Hobman JL. Metal resistance and its association with antibiotic resistance. Adv Microb Physiol. 2017;70:261-313. https://doi.org/10.1016/bs.ampbs.2017.02.001
10. Poole K. At the nexus of antibiotics and metals: the impact of Cu and Zn on antibiotic activity and resistance. Trends Microbiol. 2017;25(10):820-32. https://doi.org/10.1016/j.tim.2017.04.010
11. Perelomov L, Sizova O, Rahman MM, Perelomova I, Minkina T, Sokolov S, et al. Metal-tolerant bacteria of wastewater treatment plant in a large city. Sustainability. 2022;14(18):11335. https://doi.org/10.3390/su141811335
12. Singh S, Parihar P, Singh R, Singh VP, Prasad SM. Heavy metal tolerance in plants: role of transcriptomics, proteomics, metabolomics, and ionomics. Front Plant Sci. 2016;6:1143. https://doi.org/10.3389/fpls.2015.01143
13. Xiao X, Li W, Jin M, Zhang L, Qin L, Geng W. Responses and tolerance mechanisms of microalgae to heavy metal stress: A review. Mar Environ Res. 2023;183:105805. https://doi.org/10.1016/j.marenvres.2022.105805
14. Nanda M, Kumar V, Sharma DK. Multimetal tolerance mechanisms in bacteria: The resistance strategies acquired by bacteria that can be exploited to 'clean-up'heavy metal contaminants from water. Aquat Toxicol. 2019;212:1-10. https://doi.org/10.1016/j.aquatox.2019.04.011
15. Pal A, Bhattacharjee S, Saha J, Sarkar M, Mandal P. Bacterial survival strategies and responses under heavy metal stress: a comprehensive overview. Crit Rev Microbiol. 2022;48(3):327-355. https://doi.org/10.1080/1040841X.2021.1970512
16. Mathivanan K, Chandirika JU, Vinothkanna A, Yin H, Liu X, Meng D. Bacterial adaptive strategies to cope with metal toxicity in the contaminated environment–A review. Ecotoxicol Environ Saf. 2021;226:112863. https://doi.org/10.1016/j.ecoenv.2021.112863
17. Cabral L, Júnior GV, De Sousa ST, Dias AC, Cadete LL, Andreote FD, et al. Anthropogenic impact on mangrove sediments triggers differential responses in the heavy metals and antibiotic resistomes of microbial communities. Environ Pollut. 2016;216:460-469. https://doi.org/10.1016/j.envpol.2016.05.078

https://doi.org/10.61577/imb.2025.1000010